A Journal of the Gesellschaft Deutscher Chemiker
Angewandte Chemie
GDCh
International Edition
www.angewandte.org

Title: De-aromatization Approach Toward Superbenzoquinone Based Diradicaloid, Tetraradicaloid, and Hexaradicaloid

Authors: Jishan Wu, Guangwu Li, Yi Han, Ya Zou, Johnathan Joo Cheng Lee, and Yong Ni

To be cited as: *Angew. Chem. Int. Ed.* 10.1002/anie.201907030
Angew. Chem. 10.1002/ange.201907030

Link to VoR: http://dx.doi.org/10.1002/anie.201907030
http://dx.doi.org/10.1002/ange.201907030

WILEY-VCH

De-aromatization Approach Toward Superbenzoquinone Based Diradicaloid, Tetraradicaloid, and Hexaradicaloid

Guangwu Li,[a] Yi Han,[a] Ya Zou,[a] Johnathan Joo Cheng Lee,[a] Yong Ni,[a] and Jishan Wu*[a]

***Abstract:** We report step-by-step de-aromatization of a highly aromatic polycyclic aromatic hydrocarbon (PAH), the hexa-peri-hexabenzocoronene (also called as “superbenzene”), to give a series of superbenzoquinones containing two, four and six ketone groups. Different from traditional PAH-based quinones, these superbenzoquinones show open-shell multi-radical character via re-aromatization in the open-shell forms, which was experimentally validated by X-ray crystallographic analysis, NMR, ESR, and FT-IR measurements, and theoretically supported by restricted active space spin-flip calculations. They exhibit structure and molecular symmetry-dependent optical, electrochemical, and magnet properties.*

Introduction

De-aromatization of arenes, heteroarenes, phenols, and related substrates is an important strategy for the synthesis of complex natural products[1] and for the petroleum refinery.[2] For example, oxidative de-aromatization of the aromatic benzene ring in phenols gives *p*-benzoquinone, *o*-benzoquinone, 5-cyclohexene-1,2,3,4-tetrone, and 1,2,3,4,5,6-cyclohexanehexone (Figure 1a), which are important oxidants[3] and organic materials for such as batteries.[4] On the other hand, quinones of more extended polycyclic aromatic hydrocarbons (PAHs) are industrial vat dyes and pigments.[5] Most of these quinones have a closed-shell electronic configuration in the ground state, but some studies also demonstrated that extended *p*-benzoquinones and their analogues could show open-shell diradical character due to recovery of aromaticity of the quinoidal rings in the open-shell diradical form.[6] These open-shell diradicaloids exhibited interesting one-photon and two-photon absorption in the near-infrared (NIR) region, amphoteric redox behavior, and magnetic activity due to thermal population from singlet ground state to the low-lying triplet excited state. They are also promising ambipolar semiconductors.[7]

The quinones of PAHs are usually synthesized by direct oxidation of PAHs or Friedel-Crafts type acylation reaction,[8] and some of them have poor solubility and ill-defined structure. To attain soluble and well-defined PAH-based quinones with controlled electronic properties, it is necessary to develop efficient synthetic method. All-benzenoid PAHs are usually highly aromatic, with π-electrons preferring to localize at the individual benzene rings according to Clar’s aromatic sextet rule.[9] Therefore, they are usually very stable and have a large energy gap.[10] Hexa-*peri*-hexabenzocoronene (HBC) is a typical example, which contains seven localized aromatic sextet rings (the hexagons shaded in blue) (Figure 1b). It can be also regarded as a “superbenzene” due to its benzene-like structure with six-fold symmetry. Like the de-aromatization of benzene ring, step-by-step de-aromatization of HBC will give a series of non-aromatic superbenzoquinones containing two, four and six ketones with different symmetries (Figure 1b). Due to the highly aromatic character of HBC, these quinones have intrinsic tendency to recover aromaticity in the open-shell diradical, tetraradical and hexaradical forms (Figure 1b). Therefore, their multi-radical character and molecular symmetry-dependent electronic properties are of great interest.

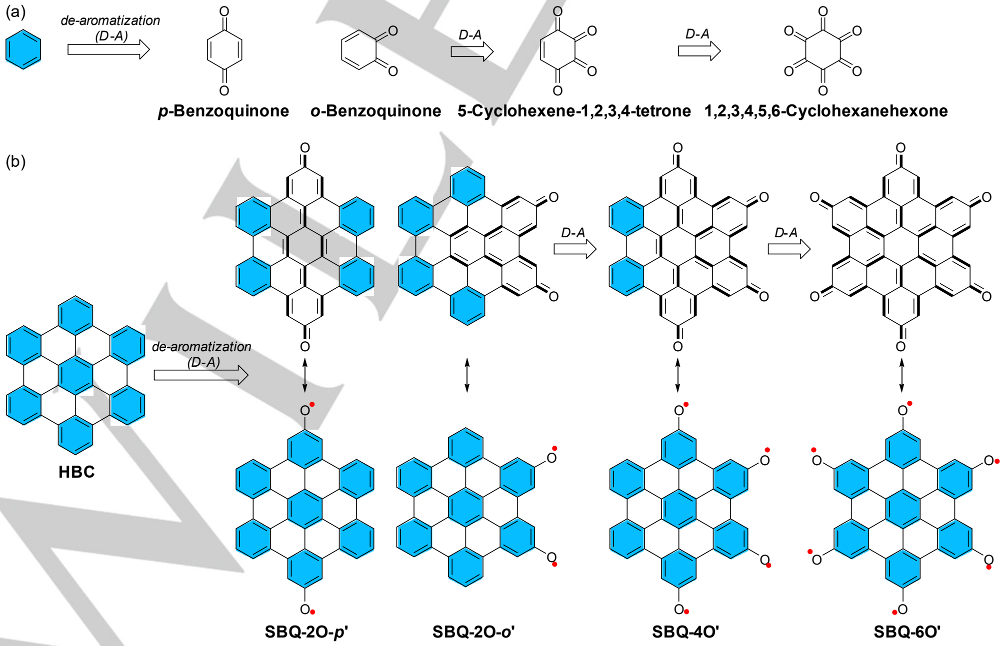

Figure 1. De-aromatization of (a) benzene and (b) hexa-*peri*-hexabenzocoronene (“superbenzene”), giving the respective benzoquinones and superbenzoquinones.

---

[a] Dr. G. Li, Y. Han, Y. Zou, J. Lee, Dr. Y. Ni, Prof. J. Wu
Department of Chemistry, National University of Singapore
3 Science Drive 3, 117543, Singapore
E-mail: chmwuj@nus.edu.sg

10.1002/anie.201907030

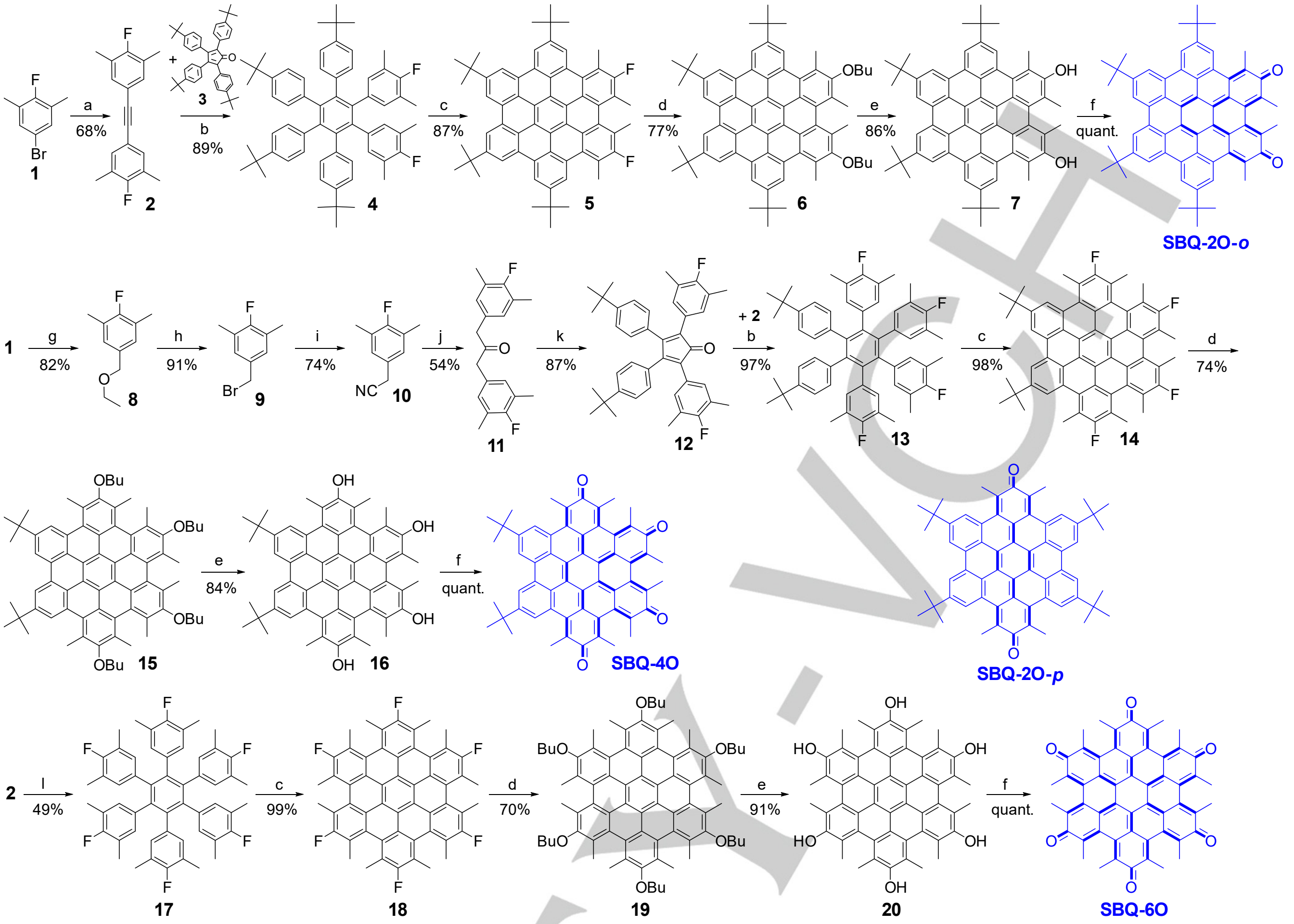

Scheme 1. Synthetic routes of **SBQ-2O-*o*, SBQ-4O** and **SBQ-6O**: (a) propiolic acid, DBU, Pd(PPh_3)$_2$$Cl_2$, dppf, DMSO, 80 °C; (b) Ph_2O, 250 °C; (c) $FeCl_3$, CH_2Cl_2, $MeNO_2$, rt; (d) *n*-BuOH, NaH, DMF, 100 °C; (e) BBr_3, CH_2Cl_2, rt; (f) PbO_2, CH_2Cl_2, rt; (g) *n*-BuLi, chloro(methoxy)ethane, THF, -78 °C; (h) HBr, CH_2Cl_2, rt; (i) NaCN, DMF, rt; (j) i) KOH, ethanol/H_2O; ii) DMAP, DCC, CH_2Cl_2, rt; (k) 1,2-bis(4-*tert*-butylphenyl)ethane-1,2-dione, KOH, ethanol, 80 °C; (l) $Co_2(CO)_8$, 1,4-dioxane, 100 °C. The strucutre of **SBQ-2O-*p*** is also shown. DBU: 1,8-Diazabicyclo[5.4.0]undec-7-ene; DMAP: 4-dimethylaminopyridine; DCC: *N,N'*-Dicyclohexylcarbodiimide.

Results and Discussion

Molecular design and synthesis. In our previous work, a *p*-benzoquinone analogue, **SBQ-2O-*p*** (Scheme 1), was synthesized and showed moderate open-shell diradical character.[11] Herein, our particular interest is to investigate the synthesis and physical properties of its *ortho*-superbenzoquinone isomer **SBQ-2O-*o***, and the further de-aromatized superbenzenetetraone **SBQ-4O** and superbenzenehexone **SBQ-6O** containing four and six ketone groups, respectively (Scheme 1). Synthesis of these compounds is challenging due to their intrinsic diraidcal or multi-radical character.[12] Compound **SBQ-2O-*p*** was previously prepared by Suzuki-Miyaura borylation followed by oxidation,[11] but this method could not be simply applied to the synthesis of these new superbenzoquinones. Alternatively, we developed a synthetic protocol mainly based nucleophilic substitution of the multifluoro-substituted HBC intermediates, followed by de-alkylation and then oxidation (Scheme 1). Two methyl- groups are placed at the *ortho*- positions of each C=O group to kinetically block the radical site (>C-O•), and *tert*-butyl groups are attached onto the backbones of the **SBQ-2O-*o*** and **SBQ-4O** to enhance solubility. In all cases, the steric hindrance between the methyl group with the neighboring methyl group or C-H bond will render the molecules into a contorted conformation, which will help to suppress unfavoured intermolecular π-π stacking.

The Pd-catalyzed tandem Sonogashira/decarboxylative reaction[13] of **1** with propiolic acid gave the 1,2-bis(4-fluoro-3,5-dimethylphenyl)ethyne **2**. Diels-Alder cycloaddition between **2** and 2,3,4,5-tetrakis(4-*tert*-butylphenyl)cyclopenta-2,4-dienone (**3**)[14] provided the hexaphenylbenzene precursor **4**, which then underwent oxidative cyclodehydrogenation with iron(III) chloride in nitromethane and dichloromethane (DCM) to afford the key HBC intermediate **5**. Nucleophilic substitution of the fluorine atoms by sodium *n*-butoxide generated the alkoxy-substituted HBC **6** and then the de-alkylation was performed by reaction with BBr_3 in DCM. The as-formed diol **7** was then oxidized into the corresponding quinone by using excessive PbO_2 in DCM in nearly quantitative conversion yield as monitored by NMR and thin-layer chromatographic analysis. Similarly, compound **SBQ-4O** was prepared from the key tetrafluoro-HBC intermediate **14**, and a difluoro- tetraphenylcyclopentadienone building block **12** had to be synthesized first *via* sequential etherification, bromination, cyanation, and condensation reaction starting from **1**. Nucleophilic substitution of **14**, de-alkylation of **15** and final oxidation of **16** gave the desired superbenzenetetrone derivative **SBQ-4O**. For the superbenzenehexone derivative **SBQ-6O**, the hexafluoro-substituted HBC intermediate **18** was first synthesized *via* $Co_2(CO)_8$-catalyzed cyclotrimerization of **2** followed by iron(III) chloride mediated cyclodehydrogenation reaction. Compound **18** has poor solubility, but after nucleophilic substitution with sodium *n*-butoxide, the product **19** shows good solubility. De-alkylation of **19** followed by oxidation afforded the desired **SBQ-6O**. The *in situ* generated compounds **SBQ-2O-*o***, **SBQ-4O** and **SBQ-6O** showed reasonable stability in solution under nitrogen protection, which allowed us to record reliable electronic absorption, FT-IR, variable-temperature (VT) ^{1}H NMR and ESR spectra, and conduct electrochemical measurements. However, the solutions in DCM underwent graduate degradation upon exposure to the ambient air and light conditions, with a half-life time of about 3.5, 10.0, and 5.2 hours, respectively, as monitored by the UV-vis-NIR absorption spectra (Figure S1 in the Supporting Information (SI)). Upon removal of the solvent under vacuum, the compounds quickly decomposed to give complicated mixture, presumably due to their radical character.

X-ray crystallographic analysis and aromaticity. Single crystals suitable for X-ray crystallographic analysis were obtained form **5**, **15**, **19** and **SBQ-6O**,[15] but compounds **SBQ-2O-*o*** and **SBQ-4O** degraded during the crystal growing. Both **5** and **15** contain paired enantiomers (*P*- and *M*- type) in the crystals due to large steric repulsion between two neighboring methyl groups at the bay region, but our attempted resolution using various chiral columns was not successful so far. The HBC backbones are severely distorted and there is no close π-π stacking. **SBQ-2O-*o*** and **SBQ-4O** are calculated to have a similar conformation to their aromatic counterparts, but the bond lengths are significantly different (Figure S14 in SI). The backbones of **19** and **SBQ-6O** show a similar highly distorted conformation, with six outermost benzenoid rings bent in an alternating up and down mode (Figure 2a-b). The distortional angle between the neighboring benzenoid rings is about 49° and 56°, respectively. Bond length analysis reveals that the rings A, B, E, G, I, L, M in **19** have a small bond length alternation (BLA) while the bonds length between those rings are much longer (Figure 2c). In addition, the harmonic oscillator model of aromaticity (HOMA)[16] values of these seven benzenoid rings (0.84~0.907) are much larger than other six-membered rings (Figure 3a). All these indicate a local aromatic character of those seven six-membered rings, which satisfies Clar's aromatic sextet rule. **SBQ-6O** has a high S_6 symmetry, and large BLA (Figure 2d) and small HOMA values (Figure 3a) were observed for each outermost six-membered rings (A′, B′, E′, G′, I′, L′, M′), in consistent with a quinoidal structure. The bond length of the C=O bonds is 1.246 Å is slightly longer than that of the closed-shell 3,3′,5,5′-tetra-*tert*-butyl-*p*-terphenoquinone (1.231 Å),[6e] indicating a major quinoidal structure with certain open-shell radical character. In addition, the calculated (B3LYP/6-31G(d)) anisotropy of induced current density (ACID)[17] plot of **19** showed seven individual clockwise diatropic ring current circuits (Figure 3b), again suggesting its local aromatic character. On the other hand, for **SBQ-6O**, there is no obvious ring current circuit (see magnified images in Figure S15 in SI). Nuclear independent chemical shift (NICS) calculations[18] (B3LYP/6-31G(d)-GIAO) indicate that more and more aromatic benzene rings are de-aromatized from **SBQ-2O-*p*** and **SBQ-2O-*o*** with four aromatic rings having a NICS(1)$_{zz}$ value below -20 ppm to the **SBQ-6O** without any aromatic ring (Figure 3c), indicating a full de-aromatization of HBC core from **19** to **SBQ-6O**.

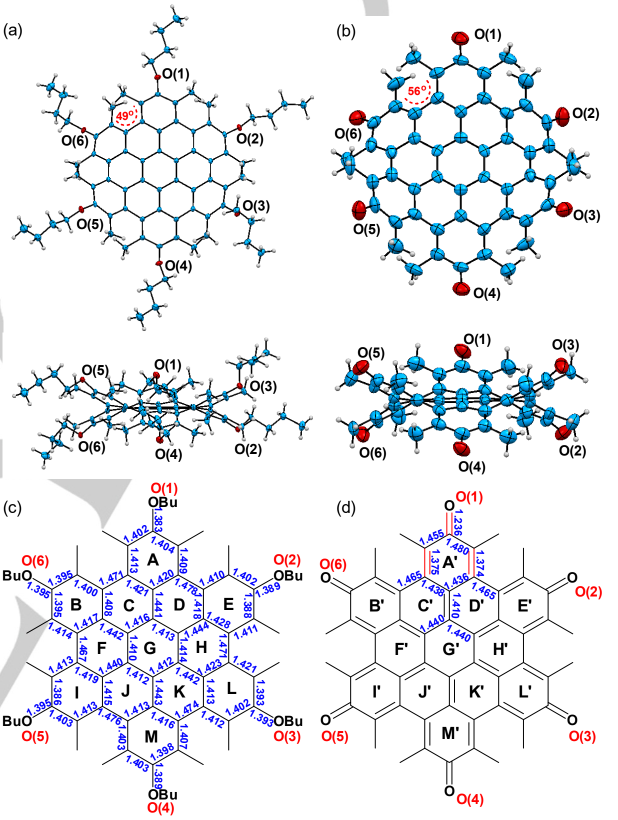

Figure 2. Top view and side view of X-ray crystallographic structures of (a) **19** and (b) **SBQ-6O**; (c) selected bond lengths (Å) of the backbones.

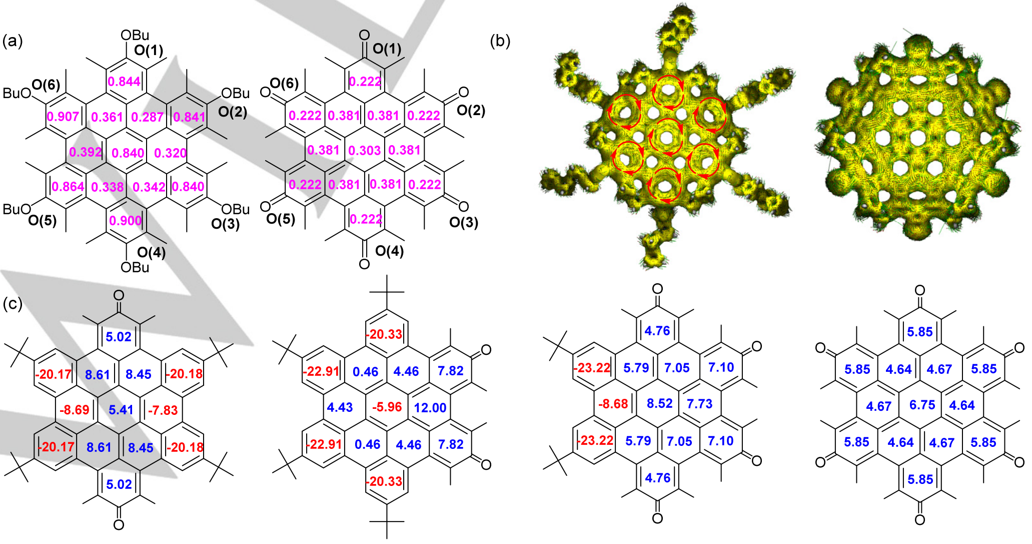

Figure 3. (a) HOMA values and (b) calculated ACID plots (isovalue: 0.03) of **19** and **SBQ-6O**; (c) calculated NICS(1)$_{zz}$ values of the four superbenzoquinones.

Magnetic properties and multi-radical character. SBQ-2O-*o* showed broaden ^{1}H NMR signals in dichloromethane-d_2 at room temperature, while decreasing the temperature led to sharpened peaks and finally the peaks became clear at 233 K (Figure 4a). This is a strong evidence that the molecule has open-shell singlet ground state and the NMR broadening is due to the thermal population of triplet species at higher temperatures.[19] For **SBQ-4O**, it displayed sharp ^{1}H NMR signals in benzene-d_6 at room temperature, while increasing the temperature led to broaden peaks (Figure 4b), indicating an open-shell singlet ground state too, but with a larger triplet excitation energy. **SBQ-6O** in THF-d_8 exhibited similar behavior, with the peak for the methyl groups partially broadened with increasing temperature (Figure S2 in SI).

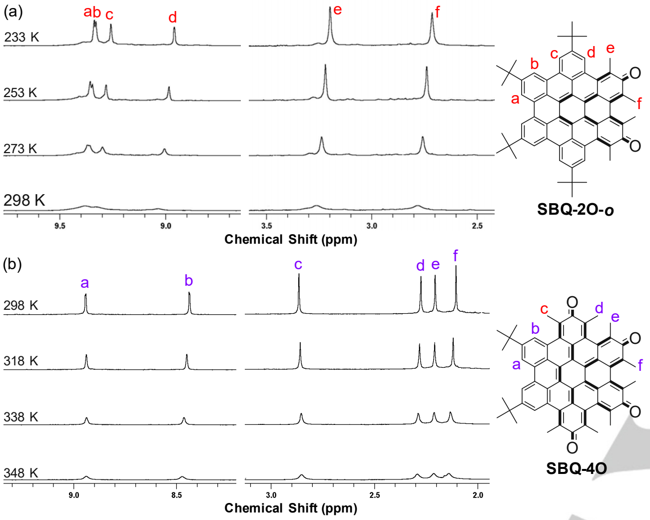

Figure 4. VT ^{1}H NMR spectra of (a) **SBQ-2O-*o*** in dichloromethane-d_2 and (b) **SBQ-4O** in benzene-d_6.

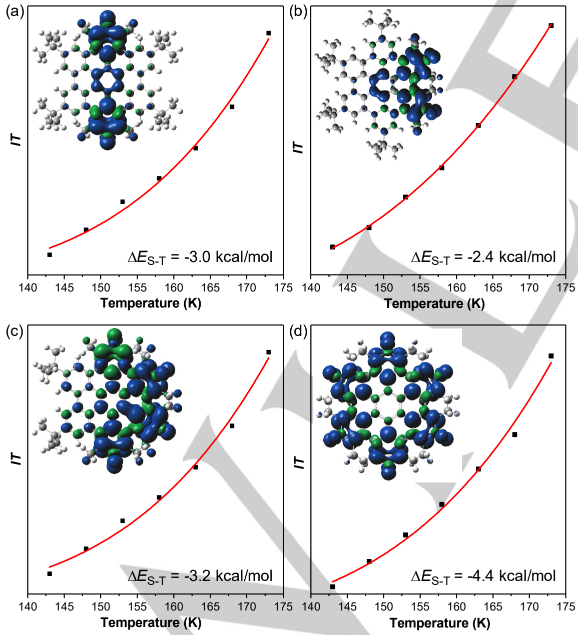

Figure 5. The fitted *IT*-*T* curves for (a) **SBQ-2O-*p***, (b) **SBQ-2O-*o***, (c) **SBQ-4O**, and (d) **SBQ-6O** based on the VT ESR data measured in the frozen solution state; *I*: integrated ESR intensity; *T*: temperature. Inset are the calculated spin density distribution maps of the triplet states.

VT ESR measurements were conducted for the freshly prepared samples in solution to further reveal their magnetic properties. A broad one-line ESR spectrum was observed for **SBQ-2O-*o***, **SBQ-4O** and **SBQ-6O** (Figure S3 in SI). The ESR intensity of the four samples decreased with decreasing temperature (Figure 5), and fitting of the data in the frozen solutions by using Bleaney–Bowers equation[20] gave a singlet–triplet energy gap ($\Delta E_{S\text{-}T}$) of -3.0, -2.4, -3.2, and -4.4 kcal/mol for **SBQ-2O-*p***, **SBQ-2O-*o***, **SBQ-4O**, and **SBQ-6O**, respectively, which is in consistent with the VT ^{1}H NMR data. The calculated (UB3LYP/6-31G(d,p)) spin density distribution maps in triplet state indicate that the spins are mainly delocalized along the extended *para* or/and *ortho* quinone moieties (inset in Figure 5).

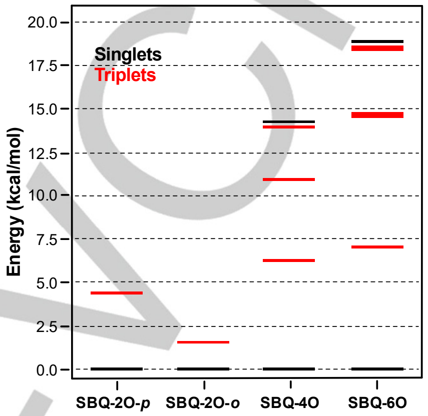

Figure 6. Calculated (RAS-SF/6-31G(d,p)) excitation energies from the singlet ground state to the triplet excited states for the four superbenzoquinones.

To further understand the electronic properties of these de-aromatized superbenzoquinones, their radical characters and vertical excitation energies were then calculated by the restricted active space spin-flip (RAS-SF) method, which has been demonstrated to be a better method than the spin-unrestricted density functional theory (DFT) to deal with the strongly correlated electron systems.[21] In all cases, the molecules have a singlet ground state (S_0), with a low-lying triplet excited state (T_1). The vertical excitation energy from S_0 to T_1 was calculated to be 4.47, 1.78, 6.72 and 7.15 kcal/mol for **SBQ-2O-*p***, **SBQ-2O-*o***, **SBQ-4O**, and **SBQ-6O**, respectively (Figure 6). This trend is in agreement with the measured $\Delta E_{S\text{-}T}$ values by VT ESR measurements. The higher triplet states (T_n) show much higher energies (> 10 kcal/mol). **SBQ-2O-*o*** exhibits the smallest S_0-T_1 vertical excitation energy than **SBQ-2O-*p***, indicating a weaker anti-ferromagnetic (AFM) coupling between the two oxygen radical centers in the *ortho* position compared to the *para* position. On the other hand, **SBQ-4O** and **SBQ-6O** with both *ortho* and *para* type spin-spin coupling show larger singlet-triplet gaps, indicating stronger AFM spin-spin coupling. The calculated frontier natural orbital profiles and the occupation numbers in their singlet ground states are shown in Figure 7. The unpaired electron densities are delocalized throughout the π-conjugated backbone, with dominant densities on the extended *para* or/and *ortho* quinone moieties. The radical character can be evaluated by the number of unpaired electrons (N_U), or the multiple diradcial character indices y_i which are defined as the occupation numbers of LUNO+*i* (i = 0, 1, 2).[22] Calculations predict that **SBQ-2O-*p*** has a smaller radical character (N_U = 1.28, y_0 = 0.641) than **SBQ-2O-*o*** (N_U = 1.34, y_0 = 0.672), in agreement with the calculated S_0-T_1 energy gaps and the VT ESR measurements. **SBQ-4O** shows occupancy at LUNO+1 and thus can be regarded as a tetraradicaloid (N_U = 1.68, y_0 = 0.470, y_1 = 0.367). **SBQ-6O** exhibits occupancy at LUNO+2 (N_U = 2.11, y_0 = 0.459, y_1 = 0.302, y_2 = 0.302) and thus can be regarded as a hexaradicaloid.

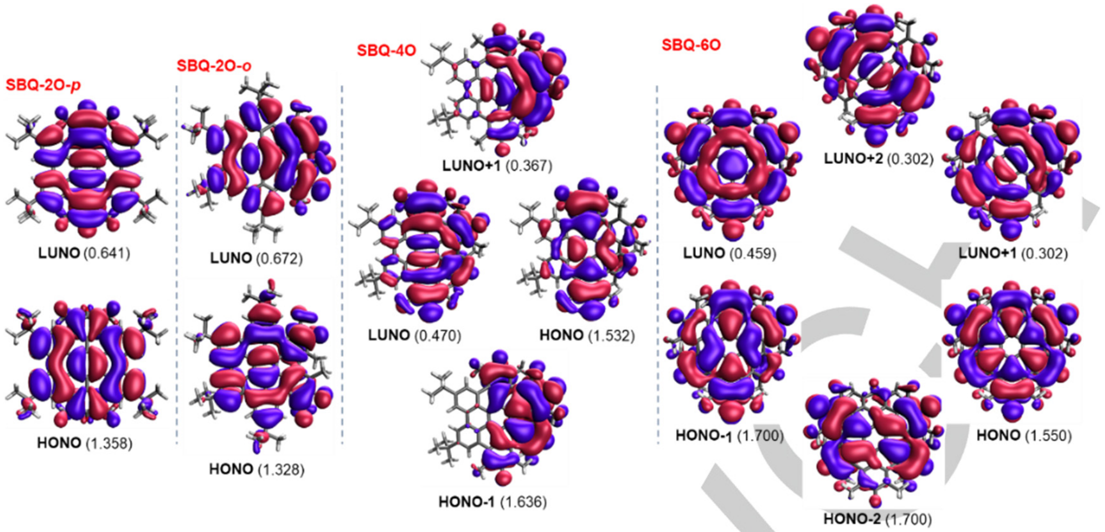

Figure 7. Calculated (RAS-SF/6-31G(d,p)) frontier natural orbitals and occupation numbers (in the parenthese) of the four superbenzoquinones in their singlet ground states.

FT IR spectra of the freshly generated **SBQ-2O-*p***, **SBQ-2O-*o*** and **SBQ-4O** were recorded in CCl_4 and while that of **SBQ-6O** was measured in THF (due to poor solubility in CCl_4). The IR band for the asymmetric stretch of C=O appeared at 1560 and 1562 cm^{-1} for **SBQ-2O-*p*** and **SBQ-2O-*o***, respectively, both are shifted to lower frequency compared to that in **SBQ-6O** (1599 cm^{-1}) (Figures S4-S5 in SI). This is in agreement with the stronger bonding interaction of the oxygen radicals in the latter as revealed by the abovementioned VT ESR measurements and RAS-SF calculations. **SBQ-4O** showed two C=O stretching band at 1590 and 1572 cm^{-1}, which are correlated to extended *ortho* and *para* quinone moiety, respectively, according to IR calculations. Again, the AFM spin-spin coupling is stronger than that in **SBQ-2O-*p*** and **SBQ-2O-*o***.

Optical and electrochemical properties. The electronic absorption spectra of the four superbenzoquinones are shown in Figure 8a for comparison. **SBQ-2O-*p*** exhibits an intense absorption band with maximum (λ_{max}) at 654 nm, which can be assigned to the HOMO→LUMO electronic transition based on time-dependent (TD) DFT calculations (Table S1 and Figures S6-S7 in SI). This HOMO→LUMO transition band shows significant red shift in **SBQ-2O-*o*** which appears at λ_{max} = 1044 nm. As shown in Figure 9, the HOMO and LUMO mainly occupy the central extended *para*-quinone moieties in **SBQ-2O-*p***, and the large spatial overlap between the HOMO and LUMO leads to a large oscillator strength (f = 0.9605). On the other hand, for **SBQ-2O-*o***, the LUMO mainly localizes at the *ortho*-quinone side, while the HOMO delocalizes through the backbone. Such partial HOMO-LUMO segregation with a charge transfer character results in a longer absorption maximum and smaller oscillator strength (f = 0.0926) (Table S2 and Figures S8-S9 in SI). For **SBQ-4O**, the HOMO and LUMO are almost fully segregated (Figure 9), leading to a nearly forbidden HOMO→LUMO transition (f = 0.0034) (Table S3 and Figures S10-S11 in SI). Accordingly, the weak absorption tail with λ_{max} = 933 nm was observed. The observed intense absorption bands at λ_{max} = 577, 692 nm can be correlated to multiple HOMO-n→LUMO+m (n=1,2; m=0,1) electronic transitions. For **SBQ-6O**, the HOMO→LUMO transition is forbidden due to its high symmetry (Tables S4 and Figures S12-S13 in SI), and thus a weak shoulder peak at 809/838 nm was found. The intense absorption band at λ_{max} = 494 nm can be assigned to HOMO-n→LUMO+m (n=1,2,3; m=1,2) electronic transitions. The trend on the observed absorption spectra of all four superbenzoquinones is in consistent with the TD-DFT calculations.

Cyclic voltammetry measurements revealed that **SBQ-2O-*p*** showed two oxidation waves with half-wave potential $E_{1/2}^{ox}$ = 0.55, 0.64 V, and one reduction wave with half-wave potential $E_{1/2}^{red}$ = -0.69 V (*vs* Fc^+/Fc) (Figure 8b). **SBQ-2O-*o*** exhibited one oxidation wave at $E_{1/2}^{ox}$ = 0.29 V, and one reduction waves at $E_{1/2}^{red}$ = -0.60 V (versus Fc^+/Fc). The electrochemical energy gap ($E_g^{EC} = E_{1/2}^{ox(1)} - E_{1/2}^{red(1)}$ = 0.89 eV) is thus smaller than that of **SBQ-2O-*p*** (1.24 eV), in consistent with the trend of optical energy gap (E_g^{Opt}: 0.97 *vs* 1.39 eV). **SBQ-4O** with four ketone groups displayed four quasi-reversible reduction waves, with $E_{1/2}^{red}$ = -0.64, -0.81, -0.96 and -1.17 V, with one irreversible oxidation wave at $E_{1/2}^{ox}$ = 0.77 V. **SBQ-6O** exhibited multiple reduction waves with $E_{1/2}^{red}$ = -43, -0.57 and -0.87 V, and two oxidation waves with $E_{1/2}^{ox}$ = 0.35 and 0.52 V. The HOMO/LUMO energy

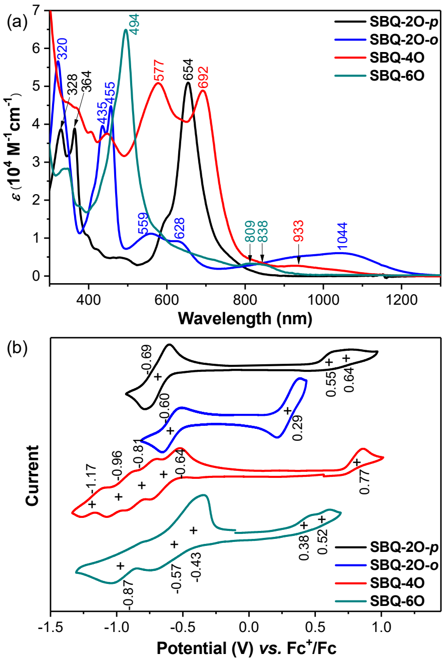

Figure 8. (a) UV-vis-NIR absorption spectra and (b) cyclic voltammograms of the four superbenzoquinones in DCM.

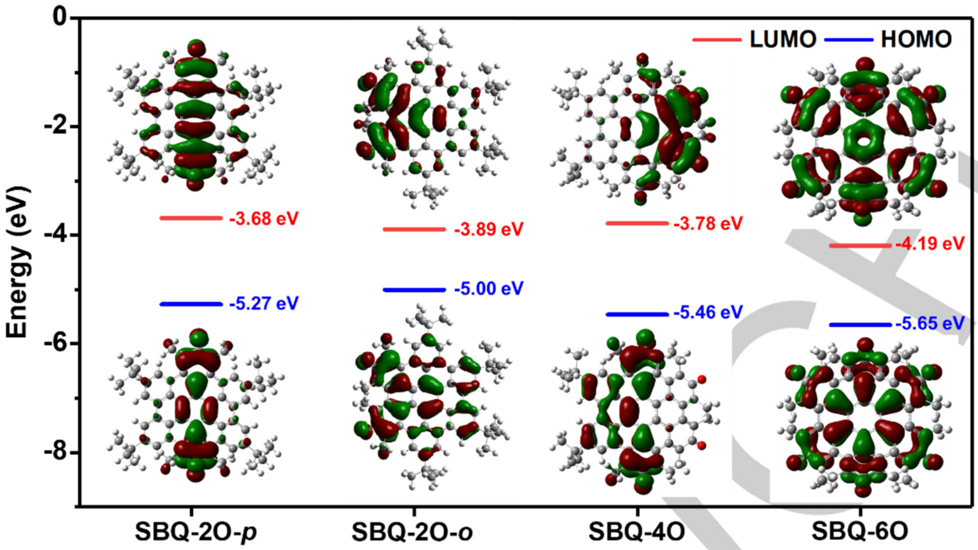

Figure 9. Calculated (B3LYP/6-31G(d,p)) frontier molecular orbitals and energy level diagrams of the four superbenzoquinones.

level was estimated to be -5.32/-4.20, -5.02/-4.29, -5.51/-4.22, and -5.11/-4.34 eV, for **SBQ-2O-*p***, **SBQ-2O-*o***, **SBQ-4O**, and **SBQ-6O**, respectively. Thus, **SBQ-6O** with six ketone groups has the lowest-lying LUMO energy level due to the high electronegativity of the C=O group. For comparison, molecules **SBQ-2O-*p***, **SBQ-2O-*o***, **SBQ-4O**, and **SBQ-6O** were calculated to have a HOMO/LUMO energy level of -5.27/-3.68, -5.00/-3.89, -5.46/-3.78, and -5.65/-4.19 eV, respectively (Figure 9), and the trend is also in agreement with the electrochemical measurements.

Conclusion

In summary, we successfully synthesized a series of superbenzoquinone-based diradicaloid, tetraradicaloid, and hexaradicaloid *via* a stepwise de-aromatization approach from the respective di-/tetra-/hexafluoro- HBC intermediates. The non-aromatic and quinoidal character of the obtained compounds was demonstrated by X-ray crystallographic analysis and theoretical calculations. These quinoidal compounds, however, have intrinsic tendency to recover aromaticity and thus display open-shell multi-radical character with magnetic activity. The radical character, singlet-triplet energy gap, optical properties, and electrochemical properties of these open-shell singlet species are dependent on the structure and molecular symmetry. Our studies provide a new synthetic method to access various PAH-based quinones with tunable physical properties and give some insights into the fundamental structure-radical character-electronic property relationships.

Acknowledgements

We acknowledge financial support from the MOE Tier 3 programme (MOE2014-T3-1-004), NRF Investigatorship (NRF-NRFI05-2019-0005) and MOE Tier 2 grant (MOE2018-T2-2-094).

Keywords: quinone • diradicaloid • polycyclic aromatic hydrocarbon • aromaticity • de-aromatization

References

[1] (a) S. P. Roche, J. A. Porco Jr., *Angew. Chem. Int. Ed.* **2011**, *50*, 4068. (b) Y. Li, S. Zhu, J. Li, A. Li, *J. Am. Chem. Soc.* **2016**, *138*, 3982. (c) G. Zhao, G. Xu, C. Qian, W. Tang, *J. Am. Chem. Soc.* **2017**, *139*, 3360.

[2] (a) C. Song, X. Ma, *Appl. Cat. B: Environ.* **2003**, *41*, 207. (b) S. Khan, S. Gupta, N. Gupt, *Biotechnol. Lett.* **2018**, *40*, 1329.

[3] (a) D. R. Buckle, "Chloranil" in *Encyclopedia of Reagents for Organic Synthesis*, **2001**, John Wiley. (b) W. Brown, A. B. Turner, *J. Chem. Soc. C: Org.* **1971**, 2566.

[4] B. Huskinson, M. P. Marshak, C. Suh, S. Er, M. R. Gerhardt, C. J. Galvin, X. Chen, A. Aspuru-Guzik, R. G. Gordon, M. J. Aziz, *Nature* **2014**, *505*, 195.

[5] (a) H. Zollinger, *Color Chemistry*, 3rd Edition, Wiley-VCH, **2001**. (b) H.-S. Bien, J. Stawitz, K. Wunderlich, *Anthraquinone dyes and intermediates, Ulmann's Encyclopedia of Industrial Chemistry*, **2012**, Vol. 3, p. 513.

[6] (a) K. Dimroth, W. Umbach, K. H. Blocher, *Angew. Chem. Int. Ed.* **1963**, *2*, 620. (b) L. A. Wendling, R. West, *J. Org. Chem.* **1978**, *43*, 1573. (c) E. D. Wellman, K. R. Lassila, R. West *J. Org. Chem.* **1984**, *49*, 965. (d) K. Takahashi, T. Suzuki, *J. Am. Chem. Soc.* **1989**, *111*, 5485. (e) R. West, J. A. Jorgenson, K. L. Stearly, J. C. Calabrese, *J. Chem. Soc., Chem. Commun.* **1991**, *2*, 1234. (f) P. Boldt, D. Bruhnke, F. Gerson, M. Scholz, P. G. Jones, F. Bar, *Helv. Chim. Acta* **1993**, *76*,1739. (g) H. Kuata, T. Tanaka, M. Oda, *Chem. Lett.* **1999**, *28*, 749. (h) T. Takahashi, K. Matsuoka, K. Takimiya, T. Otsubo, Y. Aso, *J. Am. Chem. Soc.* **2005**, *127*, 8928. (i) R. P. Ortiz, J. Casado, V. Hernández, J. T. L. Navarrete, P. M. Viruela, E. Ortí, K. Takimiya, T. Otsubo, *Angew. Chem. Int. Ed.* **2007**, *46*, 9057. (j) K. Zhang, K. Huang, J. Li, J. Luo, C. Chi, J. Wu, *Org. Lett.* **2009**, *11*, 4854. (h) S. D. Motta, F. Negri, D. Fazzi, C. Castiglioni, E. V. Canesi, *J. Phys. Chem. Lett.* **2010**, *1*, 3334. (k) A. Ueda, S. Nishida, K. Fukui, T. Ise, D. Shiomi, K. Sato, T. Takui, K. Nakasuji, Y. Morita, *Angew. Chem. Int. Ed.* **2010**, *49*, 1678. (l) E. V. Canesi, D. Fazzi, L. Colella, C. Bertarelli, C. Castiglioni, *J. Am. Chem. Soc.* **2012**, *134*, 19070. (m) D. Schmidt, M. Son, M. J. Lim, M.-J. Lin, I. Krummenacher, H. Braunschweig, D. Kim, F. Wurthner, *Angew. Chem. Int. Ed.* **2015**, *54*, 13980. (n) H. Wei, L. Zhang, H. Phan, X. Huang, T. S. Herng, J. Zhou, W. Zeng, J. Ding, S. Luo, J. Wu, Z. Zeng, *Chem. Eur. J.* **2017**, *23*, 9419. (o) K. Naoda, D. Shimizu, O. J. Kim, K. Furukawa, D. Kim, A. Osuka, *Chem. Eur. J.* **2017**, *23*, 8969. (p) S. Lee, F. Miao, H. Phan, T. S. Herng, J. Ding, J. Wu, D. Kim, *ChemPhysChem* **2017**, *18*, 591. (q) R. Rausch, D. Schmidt, D. Bialas, I. Krummenacher, H. Braunschweig, F. Würthner, *Chem. Eur. J.* **2018**, *24*, 3420-3424. (r) F. Miao, H. Phan, J. Wu, *Molecules* **2019**, *24*, 1446.

[7] (a) T. M. Pappenfus, R. J. Chesterfield, C. D. Frisbie, K. R. Mann, J. Casado, J. D. Raff and L. L. Miller, *J. Am. Chem. Soc.* **2002**, *124*, 4184. (b) R. J. Chesterfield, C. R. Newman, T. M. Pappenfus, P. C. Ewbank, M. H. Haukaas, K. R. Mann, L. L. Miller and C. D. Frisbie, *Adv. Mater.* **2003**, *15*, 1278. (c) S. Handa, E. Miyazaki, K. Takimiya and Y. Kunugi, *J. Am. Chem. Soc.* **2007**, *129*, 11684. (d) D. E. Janzen, M. W. Burand, P. C. Ewbank, T. M. Pappenfus, H. Higuchi, D. A. da Silva Filho, V. G. Young, J. L. Brédas

and K. R. Mann, *J. Am. Chem. Soc.* **2004**, *126*, 15295. (e) J. C. Ribierre, T. Fujihara, S. Watanabe, M. Matsumoto, T. Muto, A. Nakao and T. Aoyama, *Adv. Mater.* **2010**, **22**, 1722. (f) C. Zhang, X. Zhu, *Acc. Chem. Res.* **2017**, *50*, 1342. (g) D. Yuan, D. Huang, S. M. Rivero, A. Carreras, C. Zhang, Y. Zou, X. Jiao, C. R. McNeill, X. Zhu, C.-A. Di, D. Zhu, D. Casanova, J. Casado, *Chem* **2019**, *5*, 864. (h) D. Yuan, Y. Guo, Y. Zeng, Q. Fan, J. Wang, Y. Yi, X. Zhu, *Angew. Chem. Int. Ed.* **2019**, *58*, 4958.

[8] (a) S. Patai, *The Chemistry of Quinonoid Compound*; Wiley: London, **1974**. (b) Arabei, S. M.; Pavich, T. A. *J. Appl. Spectr.* **2000**, *67*, 236. (c) J. Zhang, D. Zhu, M. Matsuo, *Polymer* **2008**, *49*, 5424. (d) M. Desroches, J.-F. Morin, *Chem. Eur. J.* **2018**, *24*, 2858.

[9] (a) E. Clar, *The Aromatic Sextet*; Wiley: London, **1972**. (b) A. Konishi, Y. Hirao, M. Nakano, A. Shimizu, E. Botek, B. Champagne, D. Shiomi, K. Sato, T. Takui, K. Matsumoto, H. Kurata, T. Kubo, *J. Am. Chem. Soc.* **2010**, *132*, 11021. (c) Z. Sun, S. Lee, K. Park, X. Zhu, W. Zhang, B. Zheng, P. Hu, Z. Zeng, S. Das, Y. Li, C. Chi, R. Li, K. Huang, J. Ding, D. Kim, J. Wu, *J. Am. Chem. Soc.* **2013**, *135*, 18229.

[10] (a) J. Wu, W. Pisula, K. Müllen, *Chem. Rev.* **2007**, *107*, 718. (b) B. A. G. Hammer, K. Müllen, *Chem. Rev.* **2016**, 116, 2103. (c) M. Stępień, E. Gońka, M. Żyła, N. Sprutta, *Chem. Rev.* **2017**, 117, 3479.

[11] G. Li, H. Phan T. S. Herng, T. Y. Gopalakrishna, C. Liu, W. Zeng, J. Ding, J. Wu, *Angew. Chem. Int. Ed.* **2017**, *56*, 5012.

[12] R. Yamaguchi, S. Hiroto, H. Shinokubo, *Org. Lett.* **2012**, *14*, 2472.

[13] X. Li, F. Yang, Y. Wu, *RSC Adv.* **2014**, *4*, 13738.

[14] D. Lungerich, J. F. Hitzenberger, M. Marcia, F. Hampel, T. Drewello, N. Jux, *Angew. Chem. Int. Ed.* **2014**, *53*, 12231.

[15] CCDC no. for **5**, **15**, **19** and **SBQ-6O** are 1920677, 1920743, 1920744, and 1920745, respectively. These data are provided free of charge by The Cambridge Crystallographic Data Centre (CCDC).

[16] J. Kruszewski, T. M. Krygowski, *Tetra. Lett.* **1972**, *13*, 3839.

[17] D. Geuenich, K. Hess, F. Kohler, R. Herges, *Chem. Rev.* **2005**, *105*, 3758.

[18] P. v. R. Schleyer, C. Maerker, A. Dransfeld, H. J. Jiao, N. J. R. V. Hommes, *J. Am. Chem. Soc.* **1996**, *118*, 6317.

[19] (a) M. Abe, *Chem. Rev.* **2013**, *113*, 7011. (b) Z. Sun, Z. Zeng, J. Wu, *Acc. Chem. Res.* **2014**, *47*, 2582. (c) Z. Zeng, X. Shi, C. Chi, J. T. L. Navarrete, J. Casado, J. Wu, *Chem. Soc. Rev.* **2015**, *44*, 6578. (d) T. Kubo, *Chem. Lett.* **2015**, *44*, 111. (e) T. Y. Gopalakrishna, W. Zeng, X. Lu, J. Wu, *Chem. Commun.* **2018**, *54*, 2186.

[20] B. Bleaney, K. D. Bowers, *Proc. R. Soc. London Ser. A* **1952**, *214*, 451.

[21] (a) D. Casanova, M. Head-Gordon, *Phys. Chem. Chem. Phys.* **2009**, *11*, 9779. (b) S. Das, T. S. Herng, J. L. Zafra, P. M. Burrezo, M. Kitano, M. Ishida, T. Y. Gopalakrishna, P. Hu, A. Osuka, J. Casado, J. Ding, D. Casanova, J. Wu, *J. Am. Chem. Soc.* **2016**, *138*, 7782. (c) X. Lu, S. Lee, J. O. Kim, T. Y. Gopalakrishna, H. Phan, T. S. Herng, Z. L. Lim, Z. Zeng, J. Ding, D. Kim, J. Wu, *J. Am. Chem. Soc.* **2016**,*138*, 13048. (d) X. Lu, S. Lee, Y. Hong, H. Phan, T. Y. Gopalakrishna, T. S. Herng, T. Tanaka, M. E. Sandoval-Salinas, W. Zeng, J. Ding, D. Casanova, A. Osuka, D. Kim, J. Wu, *J. Am. Chem. Soc.* **2017**, *139*, 13173.

[22] (a) K. Yamaguchi, T. Fueno, H. Fukutome, *Chem. Phys. Lett.* **1973**, *22*, 461. (b) K. Yamaguchi, in Self-Consistent Field: Theory andApplications; Carbo, R., Klobukowski, M., Eds.; Elsevier: Amsterdam, **1990**; p 727. (c) M. Head-Gordon, *Chem. Phys. Lett.* **2003**, *372*, 508. (d) T. Minami, M. Nakano, *J. Phys. Chem. Lett.* **2012**, *3*, 145.

RESEARCH ARTICLE

From fully aromatic to fully de-aromatized superbenzene! We report stepwise de-aromatization of a superbenzene molecule to give a series of superbenzoquinones with two, four and six ketone groups. They have intrinsic tendency to recover aromaticity and thus show open-shell di-/tetra-/hexaradical character. They also exhibit geometry and molecular symmetry-dependent electronic properties.

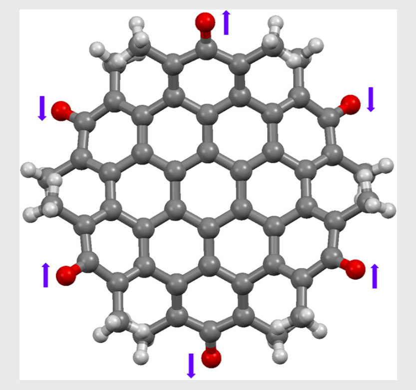

*G. Li, Y. Han, Y. Zou, J. Lee, Y. Ni, and J. Wu**

Page No. – Page No.

De-aromatization Approach Toward Superbenzoquinone Based Diradicaloid, Tetraradicaloid, and Hexaradicaloid